

Test of Lepton Flavor Universality with $B^+ \rightarrow K^+ \pi^+ \pi^- \ell^+ \ell^-$ Decays

R. Aaij *et al.**
(LHCb Collaboration)

 (Received 17 December 2024; accepted 31 March 2025; published 9 May 2025)

The first test of lepton flavor universality between muons and electrons using $B^+ \rightarrow K^+ \pi^+ \pi^- \ell^+ \ell^-$ ($\ell = e, \mu$) decays is presented. The measurement is performed with data from proton-proton collisions collected by the LHCb experiment at center-of-mass energies of 7, 8, and 13 TeV, corresponding to an integrated luminosity of 9 fb^{-1} . The ratio of branching fractions between $B^+ \rightarrow K^+ \pi^+ \pi^- e^+ e^-$ and $B^+ \rightarrow K^+ \pi^+ \pi^- \mu^+ \mu^-$ decays is measured in the dilepton invariant-mass-squared range $1.1 < q^2 < 7.0 \text{ GeV}^2/c^4$ and is found to be $R_{K\pi\pi}^{-1} = 1.31_{-0.17}^{+0.18}(\text{stat})_{-0.09}^{+0.12}(\text{syst})$, in agreement with the standard model prediction. The first observation of the $B^+ \rightarrow K^+ \pi^+ \pi^- e^+ e^-$ decay is also reported.

DOI: [10.1103/PhysRevLett.134.181803](https://doi.org/10.1103/PhysRevLett.134.181803)

In the standard model (SM) of particle physics, flavor-changing transitions between quarks of the same charge cannot occur at leading order, but only through rare loop processes involving virtual weak bosons and quarks. As arbitrarily high virtual energies become accessible within loops, new physics (NP) mediators could contribute to the decay process with comparable amplitudes to those of the SM, altering key physical observables from their expectations. Processes mediated by $b \rightarrow s \ell \ell$ quark-level transitions have drawn particular attention [1,2], notably when testing lepton flavor universality (LFU), a key property of the SM. The SM electroweak couplings are predicted to be the same for processes including e, μ , and τ leptons, after correcting for effects due to their different masses. Lepton flavor universality is an accidental symmetry of the SM, precisely verified up to 0.1% in W and Z decays [3,4], kaon and pion decays [5,6], and in decays of charmonium resonances such as the J/ψ meson [7]. However, some scenarios beyond the SM predict a violation of LFU of up to $\sim 10\%$ [8–12] in $b \rightarrow s$ transitions. Violation of LFU observed in ratios of decay rates for processes involving different lepton flavors, where uncertainties related to the hadronic form factors cancel out, would provide a model-independent signature of NP in the decay.

Several ratios testing LFU with $b \rightarrow s \ell \ell$ transitions have been measured by the BABAR [13], Belle [14], CMS [15], and LHCb Collaborations [16–24]. In this Letter, the first LFU test using $B^+ \rightarrow K^+ \pi^+ \pi^- \ell^+ \ell^-$ decays is reported, where $\ell = e, \mu$. The inclusion of

charge-conjugated processes is implied throughout. The $K^+ \pi^+ \pi^-$ hadronic system, studied at Belle [25] using $B^+ \rightarrow K^+ \pi^+ \pi^- J/\psi (\rightarrow \ell^+ \ell^-)$ decays, is populated by several intermediate states such as the $K_1(1270)^+$ and $K_1(1400)^+$ resonances, which decay predominantly via the $K^*(892)^0 \pi^+$ and $K^+ \rho(770)^0$ channels, thereby exhibiting a rich and complex spin structure. The present measurement, however, is inclusive as no resonant states are specifically identified in the hadronic system, which is selected in the $1.1 < m(K^+ \pi^+ \pi^-) < 2.4 \text{ GeV}/c^2$ kinematic region. Nevertheless, Ref. [26] shows that the result can still be interpreted in the effective field theory framework, and it thus provides independent constraints on possible extensions of the SM.

The measured observable is defined as

$$R_{K\pi\pi}^{-1} \equiv \frac{\int_{1.1 \text{ GeV}^2/c^4}^{7 \text{ GeV}^2/c^4} \frac{d\Gamma(B^+ \rightarrow K^+ \pi^+ \pi^- e^+ e^-)}{dq^2} dq^2}{\int_{1.1 \text{ GeV}^2/c^4}^{7 \text{ GeV}^2/c^4} \frac{d\Gamma(B^+ \rightarrow K^+ \pi^+ \pi^- \mu^+ \mu^-)}{dq^2} dq^2}, \quad (1)$$

where q^2 indicates the dilepton invariant-mass squared and Γ the q^2 -dependent decay rate. The measurement of the inverse ratio $R_{K\pi\pi}^{-1}$ is chosen to achieve better statistical properties given the low yield of the electron decay mode. To reduce the impact of systematic effects due to differences in the response of the LHCb detector to electrons and muons, the $R_{K\pi\pi}^{-1}$ observable is in practice measured as a double ratio, by normalizing the signal-mode branching fractions to those of the corresponding J/ψ control mode,

$$R_{K\pi\pi}^{-1} \equiv \frac{\frac{N_e(B^+ \rightarrow K^+ \pi^+ \pi^- e^+ e^-)}{N_e[B^+ \rightarrow K^+ \pi^+ \pi^- J/\psi (\rightarrow e^+ e^-)]}}{\frac{N_\mu(B^+ \rightarrow K^+ \pi^+ \pi^- \mu^+ \mu^-)}{N_\mu[B^+ \rightarrow K^+ \pi^+ \pi^- J/\psi (\rightarrow \mu^+ \mu^-)]}}, \quad (2)$$

*Full author list given at the end of the Letter.

Published by the American Physical Society under the terms of the [Creative Commons Attribution 4.0 International license](https://creativecommons.org/licenses/by/4.0/). Further distribution of this work must maintain attribution to the author(s) and the published article's title, journal citation, and DOI. Funded by SCOAP³.

where (\mathcal{N}/ϵ) are the efficiency-corrected yields. The measurement is performed using proton-proton (pp) collision data recorded by the LHCb experiment between 2011 and 2018, corresponding to integrated luminosities of 1, 2, and 6 fb^{-1} at center-of-mass energies of 7, 8, and 13 TeV, respectively. The decay $B^+ \rightarrow K^+\pi^+\pi^-\mu^+\mu^-$ has been observed at LHCb with 3 fb^{-1} of data [27], while the first observation of the $B^+ \rightarrow K^+\pi^+\pi^-e^+e^-$ mode is presented in this Letter. In addition, the $B^+ \rightarrow K^+\pi^+\pi^-J/\psi(\rightarrow \ell^+\ell^-)$ and $B^+ \rightarrow K^+\pi^+\pi^-\psi(2S)(\rightarrow \ell^+\ell^-)$ decays are used to calibrate the detector efficiencies and to validate the analysis procedure.

The LHCb detector is a single-arm forward spectrometer covering the pseudorapidity range $2 < \eta < 5$, described in detail in Refs. [28,29]. The online event selection is performed by a trigger, which consists of a hardware stage based on information from the calorimeter and muon systems, followed by a software stage which applies a full event reconstruction. At the hardware stage, events are required to have a muon with high p_T or a hadron, photon or electron with high transverse energy in the calorimeters. The software trigger requires a two-, three- or four-track secondary vertex with a significant displacement from any primary pp interaction vertex. At least one charged particle must have a large transverse momentum and be inconsistent with originating from a primary vertex. A multivariate algorithm [30,31] is used for the identification of secondary vertices consistent with the decay of a b hadron.

Simulated data samples are used to evaluate the reconstruction and selection efficiencies entering the measurement. In addition, they are used to model the reconstructed-mass line shapes for signal candidates and to estimate possible background contributions. In the simulation, pp collisions are generated using PYTHIA [32,33] with a specific LHCb configuration [34]. Decays of unstable particles are described by EvtGen [35], in which final-state radiation is generated using PHOTOS [36]. The interaction of the generated particles with the detector, and its response, are implemented using the Geant4 toolkit [37,38] as described in Ref. [39].

Simulated signal decays are generated with a uniform distribution in the phase space of the hadronic system. To reproduce the resonant structure observed in data, the simulated samples are corrected using weights computed by training a gradient-boosted decision-tree reweighter [40] on $B^+ \rightarrow K^+\pi^+\pi^-J/\psi(\rightarrow \mu^+\mu^-)$ decays. The correction uses the following quantities as inputs: the three invariant masses $m(K^+\pi^-)$, $m(\pi^+\pi^-)$, and $m(K^+\pi^+\pi^-)$, the direction of the positively charged lepton in the $\ell^+\ell^-$ rest frame, the direction of the kaon in the $K^+\pi^-$ rest frame, and the direction of the $K^+\pi^-$ system in the $K^+\pi^+\pi^-$ rest frame. The simulated samples are further corrected to account for known discrepancies between simulation and data in the B^+ kinematics and event occupancy, as well as in the track reconstruction, particle identification and trigger efficiencies.

In addition, the dilepton invariant-mass resolution is smeared to better match the data. The corrections are implemented in a similar fashion as in previous LFU measurements performed by the LHCb collaboration [22].

Candidate $B^+ \rightarrow K^+\pi^+\pi^-\ell^+\ell^-$ decays are formed from combinations of five appropriately charged tracks that originate from a common vertex. The reconstructed B^+ candidate must be compatible with originating from a pp collision when extrapolated according to its reconstructed momentum, and its decay vertex must be significantly displaced from that pp collision vertex. The final-state particles must satisfy a minimum p_T requirement and be within the acceptance of the particle identification (PID) system. Requirements on the PID-system response are also applied to discriminate between the different types of final-state particles. Electrons have a large probability to lose energy via bremsstrahlung. To mitigate such effects, reconstructed clusters in the calorimeter are added to the electron tracks if the cluster position is compatible with the extrapolated trajectory of the electron. Candidates are accepted if the reconstructed B^+ mass is in the range $[5150, 5600] \text{ MeV}/c^2$ for the electron and muon control modes and the signal muon mode, and in $[4900, 5600] \text{ MeV}/c^2$ for the signal electron mode.

To separate the signal from background composed of random combinations of tracks (combinatorial), multivariate classifiers are trained separately for decay modes containing electrons or muons. The classifiers use vertex fit chi square, alongside kinematic and topological properties of the final-state particles and of the B^+ candidate. Simulated samples are used for modeling the signal, while to model the combinatorial background, the muon classifier is trained on selected candidates with an invariant mass greater than $5600 \text{ MeV}/c^2$. A similar approach is used for the electron classifier, but, due to the smaller training dataset, events in the $[4700, 4900] \text{ MeV}/c^2$ range are also included. To prevent any bias in the training of the classifiers, the k -fold approach is used [41]. The working points of the classifiers are optimized to maximize the figure of merit $S/\sqrt{S+B}$, where S and B indicate the expected signal and background yields for a given classifier working point, respectively. As there is no *a priori* branching fraction measurement for the electron signal mode, its expected yield is instead inferred from the muon signal branching fraction assuming LFU.

The q^2 range used to select signal decays extends up to $7 \text{ GeV}^2/c^4$, above the q^2 boundary used in similar LFU tests [16–24], in order to maximize the yield of the electron mode. However, this choice leads to an increase in the number of $B^+ \rightarrow K^+\pi^+\pi^-J/\psi(\rightarrow \ell^+\ell^-)$ decays migrating into the signal region. To reduce such leakage, the invariant mass of the B^+ candidates, reconstructed by constraining the dilepton mass to the known J/ψ mass value, is required to lie outside the $[5139.3, 5476.2] \text{ MeV}/c^2$ range, which contains 95% of simulated $B^+ \rightarrow K^+\pi^+\pi^-J/\psi(\rightarrow e^+e^-)$ events.

Background arising from fully hadronic B^+ decays proceeding through an intermediate D meson, such as $B^+ \rightarrow \bar{D}^0(\rightarrow K^+\pi^-)\pi^+\pi^-\pi^+$ or $B^+ \rightarrow D^-(\rightarrow K^+\pi^-\pi^-)\pi^+\pi^+$ decays, where two pions are wrongly identified as leptons, is reduced by removing candidates where the invariant mass of the intermediate D meson, calculated by assigning the pion mass to the leptons, falls within ± 50 MeV/ c^2 of the known D meson mass [42]. Similarly, candidates arising from a swapped lepton and hadron of the same charge in $B^+ \rightarrow K^+\pi^+\pi^-J/\psi(\rightarrow \ell^+\ell^-)$ decays are removed by applying a veto on the lepton-hadron invariant mass, where the lepton mass is assigned either to the kaon or pion. Background from $B^+ \rightarrow \phi(\rightarrow K^+K^-)K^+\ell^+\ell^-$ decays where two kaons are misidentified as pions is found to be negligible. Semileptonic decays such as $B^+ \rightarrow D^-(\rightarrow K^+\pi^-\ell^+\bar{\nu}_\ell)\pi^+\ell^+\nu$ are found to already be efficiently rejected by the selection requirements. Additional requirements are implemented when selecting control $B^+ \rightarrow K^+\pi^+\pi^-J/\psi(\rightarrow \ell^+\ell^-)$ decays, to reject backgrounds from $B^+ \rightarrow K^+\psi(2S)[\rightarrow \pi^+\pi^-J/\psi(\rightarrow \ell^+\ell^-)]$ and $B^+ \rightarrow K^+\chi_{c1}(3872)[\rightarrow \pi^+\pi^-J/\psi(\rightarrow \ell^+\ell^-)]$ transitions. Less than 1% of events satisfying all selection criteria have multiple B^+ candidates. In such cases, only one candidate is retained, chosen arbitrarily. The efficiency of the above selection is observed to increase with q^2 .

Signal and control yields are extracted from unbinned maximum-likelihood fits to the invariant-mass spectrum of B^+ candidates passing the full selection. The invariant-mass resolution is improved for the control modes by constraining the dilepton mass to that of the relevant J/ψ or $\psi(2S)$ meson.

The analysis procedure is first validated by measuring $r_{J/\psi}$, the ratio of the $B^+ \rightarrow K^+\pi^+\pi^-J/\psi(\rightarrow \mu^+\mu^-)$ to $B^+ \rightarrow K^+\pi^+\pi^-J/\psi(\rightarrow e^+e^-)$ branching fractions, and $R_{\psi(2S)}$, the double ratio with the $B^+ \rightarrow K^+\pi^+\pi^-J/\psi(\rightarrow \ell^+\ell^-)$ and $B^+ \rightarrow K^+\pi^+\pi^-\psi(2S)(\rightarrow \ell^+\ell^-)$ branching fractions, constructed in the same way as Eq. (2), but with $B^+ \rightarrow K^+\pi^+\pi^-\psi(2S)(\rightarrow \ell^+\ell^-)$ decays instead of $B^+ \rightarrow K^+\pi^+\pi^-\ell^+\ell^-$ decays.

The ratio of yields of the two channels $B^+ \rightarrow K^+\pi^+\pi^-J/\psi(\rightarrow \ell^+\ell^-)$ is determined with a simultaneous fit to the invariant-mass spectra of $B^+ \rightarrow K^+\pi^+\pi^-J/\psi(\rightarrow e^+e^-)$ and $B^+ \rightarrow K^+\pi^+\pi^-J/\psi(\rightarrow \mu^+\mu^-)$ candidates, selected with $q^2 \in [7, 11]$ GeV $^2/c^4$. For these decays, the candidate- B^+ invariant-mass spectrum is modeled using a linear combination of two crystal ball (CB) functions [43]. With the core mean and resolution shared between CB functions, all line shape parameters are fixed from fits to simulated samples. However, to take into account data-simulation differences, a mean shift parameter and resolution scale factor are introduced for the fit to data. The combinatorial background component is modeled with an exponential function, with the slope parameter free to vary. After correcting for the efficiency, the $r_{J/\psi}$ ratio is found to be $r_{J/\psi} = 1.033 \pm 0.017$, where the quoted uncertainty is

statistical. No significant variation of $r_{J/\psi}$ is observed in regions (bins) of all relevant kinematical and geometrical variables, with the $r_{J/\psi}$ values found to be compatible with unity for all variables considered. Deviations from unity among the bins are retained as a systematic uncertainty on $R_{K\pi\pi}^{-1}$.

The double ratio $R_{\psi(2S)}$, is measured from an additional simultaneous fit using the pairs of decay modes $B^+ \rightarrow K^+\pi^+\pi^-J/\psi(\rightarrow \ell^+\ell^-)$ and $B^+ \rightarrow K^+\pi^+\pi^-\psi(2S)(\rightarrow \ell^+\ell^-)$, where the latter is selected with $q^2 \in [11, 15]$ GeV $^2/c^4$. The invariant-mass line shape for the $B^+ \rightarrow K^+\pi^+\pi^-\psi(2S)(\rightarrow \ell^+\ell^-)$ modes is modeled in the same way as described for the $B^+ \rightarrow K^+\pi^+\pi^-J/\psi(\rightarrow \ell^+\ell^-)$ modes. The efficiency-corrected double ratio is measured to be $R_{\psi(2S)} = 1.040 \pm 0.030$, where the quoted uncertainty is statistical. The agreement of the $r_{J/\psi}$ and $R_{\psi(2S)}$ ratios with unity is thus consistent with the expectations of LFU in charmonium decays.

The $R_{K\pi\pi}^{-1}$ observable is determined from a simultaneous fit to the invariant-mass spectra of signal $B^+ \rightarrow K^+\pi^+\pi^-\ell^+\ell^-$ and control $B^+ \rightarrow K^+\pi^+\pi^-J/\psi(\rightarrow \ell^+\ell^-)$ decays. The model describing the control component is also adopted for the signal modes, with shape parameters fixed from fits to simulated signal decays. To account for simulation-data differences a mean shift and a resolution scale factor are included. These two parameters are fixed to the values found in $B^+ \rightarrow K^+\pi^+\pi^-J/\psi(\rightarrow \ell^+\ell^-)$ decays, where the J/ψ mass constraint on the dilepton system is removed as its impact on the resolution would be inapplicable to signal. The combinatorial background is again described by an exponential function, whose slope is allowed to vary. While no other contributions are expected in the mass spectrum of $B^+ \rightarrow K^+\pi^+\pi^-\mu^+\mu^-$ decays, the lower yield and worse resolution of the $B^+ \rightarrow K^+\pi^+\pi^-e^+e^-$ mode necessitate a larger fit region, leading to the presence of additional sources of background. These include leakage from $B^+ \rightarrow K^+\pi^+\pi^-J/\psi(\rightarrow e^+e^-)$ events into the signal q^2 region; background from partially reconstructed B^+ decays, in which one or more final-state particles are not reconstructed; and residual background due to hadrons misidentified as electrons.

The mass line shape of the leakage component is modeled using simulated samples with a kernel-density estimator [44], and kept fixed in the fit. Its normalization is fixed to the yield observed in the $B^+ \rightarrow K^+\pi^+\pi^-J/\psi(\rightarrow e^+e^-)$ mode, scaled for the efficiency of the signal selection applied to the control mode.

The partially reconstructed background line shape is modeled by the convolution of an Argus function [45] with a Gaussian function. This mass line shape is fixed from a fit to data selected in the $q^2 \in [7, 11]$ GeV $^2/c^4$ region, where the control $B^+ \rightarrow K^+\pi^+\pi^-J/\psi(\rightarrow e^+e^-)$ decay mode is explicitly removed by requiring the reconstructed B^+ mass, with the dielectron mass constrained to the J/ψ meson mass, to be

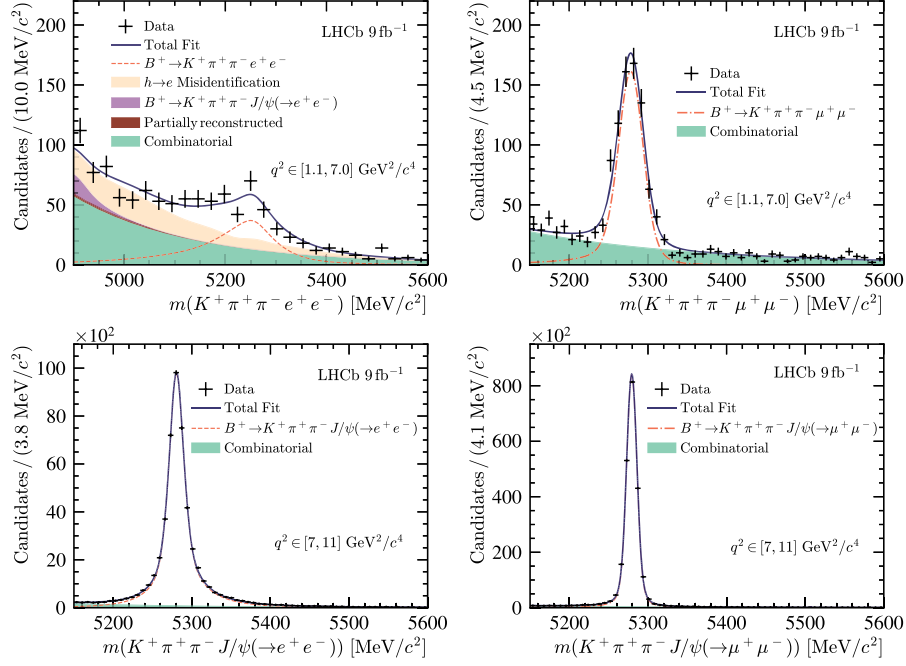


FIG. 1. Invariant-mass distributions together with the fit results of (top left) signal $B^+ \rightarrow K^+ \pi^+ \pi^- e^+ e^-$, (top right) signal $B^+ \rightarrow K^+ \pi^+ \pi^- \mu^+ \mu^-$, (bottom left) control $B^+ \rightarrow K^+ \pi^+ \pi^- J/\psi(\rightarrow e^+ e^-)$, and (bottom right) control $B^+ \rightarrow K^+ \pi^+ \pi^- J/\psi(\rightarrow \mu^+ \mu^-)$ decays, where the shaded background components are stacked.

smaller than $5150 \text{ MeV}/c^2$. The obtained sample is enriched in partially reconstructed decays as a result. The contribution from higher-mass charmonium states, such as $B^+ \rightarrow \psi(2S)(\rightarrow J/\psi \pi^+ \pi^-) K^*(892)^+(\rightarrow K^+ \pi^0)$, is then subtracted, since such feebly decays are not present for the signal decay mode. The fit is repeated without vetoing $B^+ \rightarrow K^+ \pi^+ \pi^- J/\psi(\rightarrow e^+ e^-)$ decays to extract the ratio of the remaining partially reconstructed background with respect to the control yield. This ratio ultimately constrains the relative amount of partially reconstructed background with respect to the signal yield in the fit to the signal decay mode.

The background due to hadrons misidentified as electrons is described following the procedure adopted by the LHCb Collaboration for previous LFU tests [22,23], with both its mass line shape and yield estimated directly from data. A sample of signal decays enriched in misidentified hadrons is obtained by inverting the PID requirements on the final-state electrons. The misidentified events are then weighted using misidentification rates measured in data from control channels, which allows an estimation of the amount of background candidates passing the signal selection criteria. A kernel-density estimator is used to model the mass of this background-enriched sample, whose line shape and yield are fixed in the fit to signal decays.

Results of the simultaneous fits performed to extract $R_{K\pi\pi}^{-1}$ are shown in Fig. 1. The measured signal yields are $\mathcal{N}(B^+ \rightarrow K^+ \pi^+ \pi^- e^+ e^-) = 264 \pm 21$ and $\mathcal{N}(B^+ \rightarrow K^+ \pi^+ \pi^- \mu^+ \mu^-) = 731 \pm 31$, where the uncertainties

only include the statistical component. The $R_{K\pi\pi}^{-1}$ observable is measured to be

$$R_{K\pi\pi}^{-1} = 1.31_{-0.17}^{+0.18}(\text{stat})_{-0.09}^{+0.12}(\text{syst}),$$

where the first set of uncertainties are statistical and the second systematic. The result is in agreement with the SM

TABLE I. Sources of relative systematic uncertainty considered in the measurement of $R_{K\pi\pi}^{-1}$. The contribution from each source is estimated by taking a weighted average of the systematic variations observed in each data subsample, split by data-taking period and hardware-trigger selection. To take into account correlations between subsamples, the values are scaled to the total systematic uncertainty obtained from the fit procedure, where the likelihood is convolved with a Gaussian distribution, with width equal to the quadratic sum of the systematic uncertainties for all sources considered. The total is evaluated by summing the different sources in quadrature.

Source	Uncertainty [%]
$r_{J/\psi}$ nonflatness	[−1.2, +1.6]
Efficiency calibration	[−1.8, +2.4]
Phase-space simulation	[−3.0, +4.0]
Fit bias	[−1.1, +1.4]
Signal line shape	[−1.7, +2.2]
Leakage from resonant decays	[−1.0, +1.4]
Hadron-to-electron misidentification	[−5.3, +7.1]
Partially reconstructed background	[−0.9, +1.2]
Total	[−6.9, +9.2]

expectation of LFU at the level of 1.7 standard deviations (σ). The significance of the $B^+ \rightarrow K^+\pi^+\pi^-e^+e^-$ decay is evaluated with Wilks' theorem [46] and found to exceed 10σ , including both statistical and systematic uncertainties, confirming the first observation for the signal dielectron channel. The behavior of the likelihood profile is shown in Fig. 2, indicating the absence of other local minima.

Table I summarizes all sources of systematic uncertainty considered. Systematic uncertainties associated with the efficiencies are evaluated for each correction applied to the simulated samples by using different input variables for the training of the reweighters or by using different decay modes as calibration samples. The correction of the phase-space model is the dominant systematic source related to the efficiencies. This systematic uncertainty is evaluated by training the reweighter on $B^+ \rightarrow K^+\pi^+\pi^-\gamma$ instead of $B^+ \rightarrow K^+\pi^+\pi^-J/\psi(\rightarrow \mu^+\mu^-)$ decays, assessing the effects of training the phase-space corrections at lower q^2 values as opposed to higher. Additional systematic uncertainties are assigned by training the reweighter on simulated signal samples where the $K^+\pi^+\pi^-$ hadronic system is arbitrarily generated with several spin configurations.

The fit results are validated using an ensemble of pseudoexperiments generated from the nominal fit results. Subsequent fits of the pseudoexperiments are found to provide good statistical coverage, though with a small bias retained as a systematic uncertainty. Additional systematic uncertainties are assigned due to the modeling of components contributing to the invariant-mass spectrum, which might affect the estimation of signal yields. These are evaluated with the same pseudoexperiments used to assess the fit bias, refitting when varying the line shape or amount of a given fit component. The dominant systematic source of this type is related to the data-driven estimation of the background shape due the misidentification of hadrons as electrons. To determine this systematic uncertainty, the model used in the background-enriched sample is varied with an alternative empirical line shape consisting of the linear combination of two Gaussian functions with one exponential function. The uncertainty from the signal line shape is determined by fluctuating its shape parameters around the fixed values of the nominal fit. To assess the systematic uncertainty related to leakage from $B^+ \rightarrow K^+\pi^+\pi^-J/\psi(\rightarrow e^+e^-)$ decays into the signal sample, the yield of the leakage component is allowed to vary within its uncertainty obtained from simulation. Finally, uncertainties induced by the partially reconstructed background model are evaluated using an alternative model that is derived fully from simulation. Furthermore, in order to relax the Gaussian constraint relating the amounts of partially reconstructed background between signal and control decays, the Gaussian width is scaled by 150% and the fit repeated, assigning the difference as a systematic uncertainty.

In summary, this Letter presents the first inclusive LFU test using $B^+ \rightarrow K^+\pi^+\pi^-\ell^+\ell^-$ decays. Since the electron-mode measurement is statistically limited, further improvements are to be expected with the new dataset being collected with the LHCb detector. With 9 fb^{-1} of data, the measured value for $R_{K\pi\pi}^{-1}$ is found to be compatible with the SM expectation of LFU at the 1.7σ level. These results provide independent constraints on possible LFU-violating extensions of the SM. The first observation of the $B^+ \rightarrow K^+\pi^+\pi^-e^+e^-$ decay is also reported.

Acknowledgments—We express our gratitude to our colleagues in the CERN accelerator departments for the excellent performance of the LHC. We thank the technical and administrative staff at the LHCb institutes. We acknowledge support from CERN and from the national agencies: ARC (Australia); CAPES, CNPq, FAPERJ and FINEP (Brazil); MOST and NSFC (China); CNRS/IN2P3 (France); BMBF, DFG and MPG (Germany); INFN (Italy); NWO (Netherlands); MNiSW and NCN (Poland); MCID/IFA (Romania); MSHE (Russia); MICIU and AEI (Spain); SNSF and SER (Switzerland); NASU (Ukraine); STFC (United Kingdom); DOE NP and NSF (USA). We acknowledge the computing resources that are provided by ARDC (Australia), CBPF (Brazil), CERN, IHEP and LZU (China), IN2P3 (France), KIT and DESY (Germany), INFN (Italy), SURF (Netherlands), Polish WLCG (Poland), IFIN-HH (Romania), PIC (Spain), CSCS (Switzerland), and GridPP (United Kingdom). We are indebted to the communities behind the multiple open-source software packages on which we depend. Individual groups or members have received support from Key Research Program of Frontier Sciences of CAS, CAS PIFI, CAS CCEPP, Fundamental Research Funds for the Central Universities, and Sci. & Tech. Program of Guangzhou (China); Minciencias (Colombia); EPLANET, Marie Skłodowska-Curie Actions, ERC and NextGenerationEU (European Union); A*MIDEX, ANR, IPhU and Labex P2IO, and Région Auvergne-Rhône-Alpes (France); Alexander-von-Humboldt Foundation (Germany); ICSC (Italy); Severo Ochoa and María de Maeztu Units of Excellence, GVA, XuntaGal, GENCAT, InTalent-Inditex and Prog. Atracción Talento CM (Spain); SRC (Sweden); the Leverhulme Trust, the Royal Society and UKRI (United Kingdom).

Data availability—The data that support the findings of this article are openly available [47].

-
- [1] Y. Wang and D. Atwood, Rate difference between $b \rightarrow s\mu^+\mu^-$ and $b \rightarrow se^+e^-$ in supersymmetry with large $\tan\beta$, *Phys. Rev. D* **68**, 094016 (2003).
 - [2] G. Hiller and F. Krüger, More model-independent analysis of $b \rightarrow s$ processes, *Phys. Rev. D* **69**, 074020 (2004).

- [3] S. Schael *et al.* (ALEPH, DELPHI, L3, OPAL Collaborations and LEP Electroweak Working Group), Electroweak measurements in electron–positron collisions at W-boson-pair energies at LEP, *Phys. Rep.* **532**, 119 (2013).
- [4] S. Schael *et al.* (ALEPH, DELPHI, L3, OPAL, and SLD Collaborations, LEP Electroweak Working Group, SLD Electroweak and Heavy Flavour Groups), Precision electroweak measurements on the Z resonance, *Phys. Rep.* **427**, 257 (2006).
- [5] A. Aguilar-Arevalo *et al.* (PiENU Collaboration), Improved measurement of the $\pi \rightarrow e\nu$ branching ratio, *Phys. Rev. Lett.* **115**, 071801 (2015).
- [6] C. Lazzeroni *et al.* (NA62 Collaboration), Precision measurement of the ratio of the charged kaon leptonic decay rates, *Phys. Lett. B* **719**, 326 (2013).
- [7] V. M. Aulchenko *et al.* (KEDR Collaboration), Measurement of the ratio of the lepton widths $\Gamma_{ee}/\Gamma_{\mu\mu}$ for the J/ψ meson, *Phys. Lett. B* **731**, 227 (2014).
- [8] R. Barbieri, C. W. Murphy, and F. Senia, B-decay anomalies in a composite leptoquark model, *Eur. Phys. J. C* **77**, 8 (2017).
- [9] W. Altmannshofer, S. Gori, M. Pospelov, and I. Yavin, Quark flavor transitions in $L_\mu - L_\tau$ models, *Phys. Rev. D* **89**, 095033 (2014).
- [10] A. Crivellin, G. D’Ambrosio, and J. Heeck, Explaining $h \rightarrow \mu^\pm \tau^\mp$, $B \rightarrow K^{*0} \mu^+ \mu^-$, and $B \rightarrow K \mu^+ \mu^- / B \rightarrow K e^+ e^-$ in a two-Higgs-doublet model with gauged $L_\mu - L_\tau$, *Phys. Rev. Lett.* **114**, 151801 (2015).
- [11] A. Celis, J. Fuentes-Martín, M. Jung, and H. Serôdio, Family nonuniversal Z' models with protected flavor-changing interactions, *Phys. Rev. D* **92**, 015007 (2015).
- [12] A. Falkowski, M. Nardecchia, and R. Ziegler, Lepton flavor non-universality in B-meson decays from a U(2) flavor model, *J. High Energy Phys.* **11** (2015) 173.
- [13] J. P. Lees *et al.* (BABAR Collaboration), Measurement of branching fractions and rate asymmetries in the rare decays $B \rightarrow K^{(*)} \ell^+ \ell^-$, *Phys. Rev. D* **86**, 032012 (2012).
- [14] S. Choudhury *et al.* (Belle Collaboration), Test of lepton flavor universality and search for lepton flavor violation in $B \rightarrow K \ell^+ \ell^-$ decays, *J. High Energy Phys.* **03** (2021) 105.
- [15] A. Hayrapetyan *et al.* (CMS Collaboration), Test of lepton flavor universality in $B^\pm \rightarrow K^\pm \mu^+ \mu^-$ and $B^\pm \rightarrow K^\pm e^+ e^-$ decays in proton-proton collisions at $\sqrt{s} = 13$ TeV, *Rep. Prog. Phys.* **87**, 077802 (2024).
- [16] R. Aaij *et al.* (LHCb Collaboration), Test of lepton universality using $B^+ \rightarrow K^+ \ell^+ \ell^-$ decays, *Phys. Rev. Lett.* **113**, 151601 (2014).
- [17] R. Aaij *et al.* (LHCb Collaboration), Test of lepton universality with $B^0 \rightarrow K^{*0} \ell^+ \ell^-$ decays, *J. High Energy Phys.* **08** (2017) 055.
- [18] R. Aaij *et al.* (LHCb Collaboration), Search for lepton-universality violation in $B^+ \rightarrow K^+ \ell^+ \ell^-$ decays, *Phys. Rev. Lett.* **122**, 191801 (2019).
- [19] R. Aaij *et al.* (LHCb Collaboration), Test of lepton universality using $\Lambda_b^0 \rightarrow p K^- \ell^+ \ell^-$ decays, *J. High Energy Phys.* **05** (2020) 040.
- [20] R. Aaij *et al.* (LHCb Collaboration), Test of lepton universality in beauty-quark decays, *Nat. Phys.* **18**, 277 (2022).
- [21] R. Aaij *et al.* (LHCb Collaboration), Tests of lepton universality using $B^0 \rightarrow K_S^0 \ell^+ \ell^-$ and $B^+ \rightarrow K^{*+} \ell^+ \ell^-$ decays, *Phys. Rev. Lett.* **128**, 191802 (2022).
- [22] R. Aaij *et al.* (LHCb Collaboration), Measurement of lepton universality parameters in $B^+ \rightarrow K^+ \ell^+ \ell^-$ and $B^0 \rightarrow K^{*0} \ell^+ \ell^-$ decays, *Phys. Rev. D* **108**, 032002 (2023).
- [23] R. Aaij *et al.* (LHCb Collaboration), Test of lepton universality in $b \rightarrow s \ell^+ \ell^-$ decays, *Phys. Rev. Lett.* **131**, 051803 (2023).
- [24] R. Aaij *et al.* (LHCb Collaboration), Test of lepton flavour universality with $B_S^0 \rightarrow \phi \ell^+ \ell^-$ decays, *Phys. Rev. Lett.* **134**, 121803 (2025).
- [25] H. Guler *et al.* (Belle Collaboration), Study of the $K^+ \pi^+ \pi^-$ final state in $B^+ \rightarrow J/\psi K^+ \pi^+ \pi^-$ and $B^+ \rightarrow \psi' K^+ \pi^+ \pi^-$, *Phys. Rev. D* **83**, 032005 (2011).
- [26] G. Isidori, D. Lancierini, A. Mathad, P. Owen, N. Serra, and R. S. Coutinho, A general effective field theory description of $b \rightarrow s \ell \ell$ lepton universality ratios, *Phys. Lett. B* **830**, 137151 (2022).
- [27] R. Aaij *et al.* (LHCb Collaboration), First observations of the rare decays $B^+ \rightarrow K^+ \pi^+ \pi^- \mu^+ \mu^-$ and $B^+ \rightarrow \phi K^+ \mu^+ \mu^-$, *J. High Energy Phys.* **10** (2014) 064.
- [28] A. A. Alves, Jr. *et al.* (LHCb Collaboration), The LHCb detector at the LHC, *J. Instrum.* **3**, S08005 (2008).
- [29] R. Aaij *et al.* (LHCb Collaboration), LHCb detector performance, *Int. J. Mod. Phys. A* **30**, 1530022 (2015).
- [30] V. V. Gligorov and M. Williams, Efficient, reliable and fast high-level triggering using a bonsai boosted decision tree, *J. Instrum.* **8**, P02013 (2013).
- [31] T. Likhomanenko, P. Ilten, E. Khairullin, A. Rogozhnikov, A. Ustyuzhanin, and M. Williams, LHCb topological trigger reoptimization, *J. Phys. Conf. Ser.* **664**, 082025 (2015).
- [32] T. Sjöstrand, S. Mrenna, and P. Skands, A brief introduction to PYTHIA 8.1, *Comput. Phys. Commun.* **178**, 852 (2008).
- [33] T. Sjöstrand, S. Mrenna, and P. Skands, PYTHIA 6.4 physics and manual, *J. High Energy Phys.* **05** (2006) 026.
- [34] I. Belyaev *et al.*, Handling of the generation of primary events in gauss, the LHCb simulation framework, *J. Phys. Conf. Ser.* **331**, 032047 (2011).
- [35] D. J. Lange, The EvtGen particle decay simulation package, *Nucl. Instrum. Methods Phys. Res., Sect. A* **462**, 152 (2001).
- [36] N. Davidson, T. Przedzinski, and Z. Was, PHOTOS interface in C++: Technical and physics documentation, *Comput. Phys. Commun.* **199**, 86 (2016).
- [37] J. Allison *et al.* (Geant4 Collaboration), Geant4 developments and applications, *IEEE Trans. Nucl. Sci.* **53**, 270 (2006).
- [38] S. Agostinelli *et al.* (Geant4 Collaboration), Geant4: A simulation toolkit, *Nucl. Instrum. Methods Phys. Res., Sect. A* **506**, 250 (2003).
- [39] M. Clemencic, G. Corti, S. Easo, C. R. Jones, S. Miglioranza, M. Pappagallo, and P. Robbe, The LHCb simulation application, gauss: Design, evolution and experience, *J. Phys. Conf. Ser.* **331**, 032023 (2011).
- [40] A. Rogozhnikov, Reweighting with boosted decision trees, *J. Phys. Conf. Ser.* **762**, 012036 (2016).
- [41] A. Blum, A. Kalai, and J. Langford, Beating the hold-out: Bounds for k-fold and progressive cross-validation, in *Proceedings of the Twelfth Annual Conference on*

Computational Learning Theory, COLT '99 (Association for Computing Machinery, New York, NY, 1999), pp. 203–208.

- [42] S. Navas *et al.* (Particle Data Group), Review of particle physics, *Phys. Rev. D* **110**, 030001 (2024).
 [43] T. Skwarnicki, A study of the radiative cascade transitions between the upsilon-prime and upsilon resonances, Ph.D. thesis, Institute of Nuclear Physics, Krakow, 1986, DESY-F31-86-02.

- [44] K. Cranmer, Kernel estimation in high-energy physics, *Comput. Phys. Commun.* **136**, 198 (2001).
 [45] H. Albrecht *et al.*, Search for hadronic $b \rightarrow u$ decays, *Phys. Lett. B* **241**, 278 (1990).
 [46] S. S. Wilks, The large-sample distribution of the likelihood ratio for testing composite hypotheses, *Ann. Math. Stat.* **9**, 60 (1938).
 [47] Data associated with the plots in this publication, <https://cds.cern.ch/record/2919997/>.

End Matter

Figure 2 shows twice the negative log-likelihood profile scan from the maximum-likelihood fit used to extract $R_{K\pi\pi}^{-1}$. The likelihood profile includes systematic uncertainties, which are added directly in the fit

procedure by convolving the likelihood with a Gaussian distribution, with width equal to the quadratic sum of the systematic uncertainties considered.

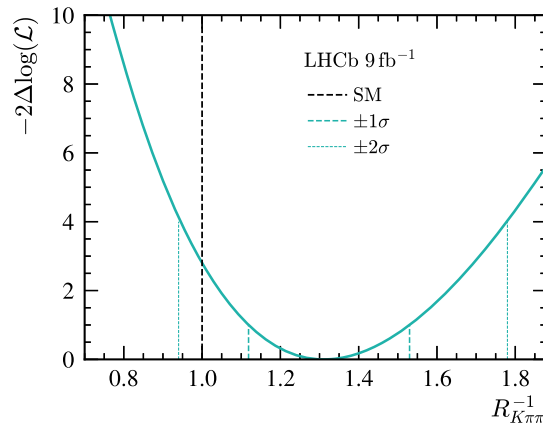


FIG. 2. Difference in twice the negative log-likelihood when varying $R_{K\pi\pi}^{-1}$ with respect to the fitted value.

R. Aaij³⁸, A. S. W. Abdelmotteleb⁵⁷, C. Abellan Beteta⁵¹, F. Abudinén⁵⁷, T. Ackernley⁶¹, A. A. Adefisoye⁶⁹, B. Adeva⁴⁷, M. Adinolfi⁵⁵, P. Adlarson⁸², C. Agapopoulou¹⁴, C. A. Aidala⁸³, Z. Ajaltouni¹¹, S. Akar¹¹, K. Akiba³⁸, P. Albicocco²⁸, J. Albrecht^{19,b}, F. Alessio⁴⁹, M. Alexander⁶⁰, Z. Aliouche⁶³, P. Alvarez Cartelle⁵⁶, R. Amalric¹⁶, S. Amato³, J. L. Amey⁵⁵, Y. Amhis¹⁴, L. An⁶, L. Anderlini²⁷, M. Andersson⁵¹, A. Andreianov⁴⁴, P. Andreola⁵¹, M. Andreotti²⁶, D. Andreou⁶⁹, A. Anelli^{31,49,c}, D. Ao⁷, F. Archilli^{37,d}, M. Argenton²⁶, S. Arguedas Cuendis^{9,49}, A. Artamonov⁴⁴, M. Artuso⁶⁹, E. Aslanides¹³, R. Ataíde Da Silva⁵⁰, M. Atzeni⁶⁵, B. Audurier¹², D. Bacher⁶⁴, I. Bachiller Perea¹⁰, S. Bachmann²², M. Bachmayer⁵⁰, J. J. Back⁵⁷, P. Baladron Rodriguez⁴⁷, V. Balagura¹⁵, A. Balboni²⁶, W. Baldini²⁶, L. Balzani¹⁹, H. Bao⁷, J. Baptista de Souza Leite⁶¹, C. Barbero Pretel^{47,12}, M. Barbetti²⁷, I. R. Barbosa⁷⁰, R. J. Barlow⁶³, M. Barnyakov²⁵, S. Barsuk¹⁴, W. Barter⁵⁹, J. Bartz⁶⁹, J. M. Basels¹⁷, S. Bashir⁴⁰, G. Bassi^{35,e}, B. Batsukh⁵, P. B. Battista¹⁴, A. Bay⁵⁰, A. Beck⁵⁷, M. Becker¹⁹, F. Bedeschi³⁵, I. B. Bediaga², N. A. Behling¹⁹, S. Belin⁴⁷, K. Belous⁴⁴, I. Belov²⁹, I. Belyaev³⁶, G. Benane¹³, G. Bencivenni²⁸, E. Ben-Haim¹⁶, A. Berezhnoy⁴⁴, R. Bernet⁵¹, S. Bernet Andres⁴⁵, A. Bertolin³³, C. Betancourt⁵¹, F. Betti⁵⁹, J. Bex⁵⁶, Ia. Bezshyiko⁵¹, J. Bhom⁴¹, M. S. Bieker¹⁹, N. V. Biesuz²⁶, P. Billoir¹⁶, A. Biolchini³⁸, M. Birch⁶², F. C. R. Bishop¹⁰, A. Bitadze⁶³, A. Bizzeti¹⁹, T. Blake⁵⁷, F. Blanc⁵⁰, J. E. Blank¹⁹, S. Blusk⁶⁹, V. Bocharnikov⁴⁴, J. A. Boelhaeve¹⁹, O. Boente Garcia¹⁵, T. Boettcher⁶⁶, A. Bohare⁵⁹, A. Boldyrev⁴⁴, C. S. Bolognani⁷⁹

- R. Bolzonella^{26,f} R. B. Bonacci¹ N. Bondar⁴⁴ A. Bordelius⁴⁹ F. Borgato^{33,g} S. Borghi⁶³ M. Borsato^{31,c}
 J. T. Borsuk⁴¹ E. Bottalico⁶¹ S. A. Bouchiba⁵⁰ M. Bovill⁶⁴ T. J. V. Bowcock⁶¹ A. Boyer⁴⁹ C. Bozzi²⁶
 J. D. Brandenburg⁸⁴ A. Brea Rodriguez⁵⁰ N. Breer¹⁹ J. Brodzicka⁴¹ A. Brossa Gonzalo^{47,a} J. Brown⁶¹
 D. Brundu³² E. Buchanan⁵⁹ L. Buonincontri^{33,g} M. Burgos Marcos⁷⁹ A. T. Burke⁶³ C. Burr⁴⁹ J. S. Butter⁵⁶
 J. Buytaert⁴⁹ W. Byczynski⁴⁹ S. Cadeddu³² H. Cai⁷⁴ A. C. Caillet¹⁶ R. Calabrese^{26,f} S. Calderon Ramirez⁹
 L. Calefice⁴⁶ S. Cali²⁸ M. Calvi^{31,c} M. Calvo Gomez⁴⁵ P. Camargo Magalhaes^{2,h} J. I. Cambon Bouzas⁴⁷
 P. Campana²⁸ D. H. Campora Perez⁷⁹ A. F. Campoverde Quezada⁷ S. Capelli³¹ L. Capriotti²⁶
 R. Caravaca-Mora⁹ A. Carbone^{25,i} L. Carcedo Salgado⁴⁷ R. Cardinale^{29,j} A. Cardini³² P. Carniti^{31,c}
 L. Carus²² A. Casais Vidal⁶⁵ R. Caspary²² G. Casse⁶¹ M. Cattaneo⁴⁹ G. Cavallero^{26,49} V. Cavallini^{26,f}
 S. Celani²² S. Cesare^{30,k} A. J. Chadwick⁶¹ I. Chahrour⁸³ M. Charles¹⁶ Ph. Charpentier⁴⁹
 E. Chatzianagnostou³⁸ M. Chefdeville¹⁰ C. Chen¹³ S. Chen⁵ Z. Chen⁷ A. Chernov⁴¹ S. Chernyshenko⁵³
 X. Chiotopoulos⁷⁹ V. Chobanova⁸¹ M. Chrzaszcz⁴¹ A. Chubykin⁴⁴ V. Chulikov²⁸ P. Ciambrone²⁸
 X. Cid Vidal⁴⁷ G. Ciezarek⁴⁹ P. Cifra⁴⁹ P. E. L. Clarke⁵⁹ M. Clemencic⁴⁹ H. V. Cliff⁵⁶ J. Closier⁴⁹
 C. Cocha Toapaxi²² V. Coco⁴⁹ J. Cogan¹³ E. Cogneras¹¹ L. Cojocariu⁴³ S. Collaviti⁵⁰ P. Collins⁴⁹
 T. Colombo⁴⁹ M. Colonna¹⁹ A. Comerma-Montells⁴⁶ L. Congedo²⁴ A. Contu³² N. Cooke⁶⁰ I. Corredoira⁴⁷
 A. Correia¹⁶ G. Corti⁴⁹ J. J. Cottee Meldrum⁵⁵ B. Couturier⁴⁹ D. C. Craik⁵¹ M. Cruz Torres^{2,l}
 E. Curras Rivera⁵⁰ R. Currie⁵⁹ C. L. Da Silva⁶⁸ S. Dadabaev⁴⁴ L. Dai⁷¹ X. Dai⁴ E. Dall'Occo⁴⁹
 J. Dalseno⁴⁷ C. D'Ambrosio⁴⁹ J. Daniel¹¹ A. Danilina⁴⁴ P. d'Argent²⁴ G. Darze³ A. Davidson⁵⁷
 J. E. Davies⁶³ A. Davis⁶³ O. De Aguiar Francisco⁶³ C. De Angelis^{32,m} F. De Benedetti⁴⁹ J. de Boer³⁸
 K. De Bruyn⁷⁸ S. De Capua⁶³ M. De Cian²² U. De Freitas Carneiro Da Graca^{2,n} E. De Lucia²⁸
 J. M. De Miranda² L. De Paula³ M. De Serio^{24,o} P. De Simone²⁸ F. De Vellis¹⁹ J. A. de Vries⁷⁹
 F. Debernardis²⁴ D. Decamp¹⁰ V. Dedu¹³ S. Dekkers¹ L. Del Buono¹⁶ B. Delaney⁶⁵ H.-P. Dembinski¹⁹
 J. Deng⁸ V. Denysenko⁵¹ O. Deschamps¹¹ F. Dettori^{32,m} B. Dey⁷⁷ P. Di Nezza²⁸ I. Diachkov⁴⁴
 S. Didenko⁴⁴ S. Ding⁶⁹ L. Dittmann²² V. Dobishuk⁵³ A. D. Docheva⁶⁰ C. Dong^{4,p} A. M. Donohoe²³
 F. Dordei³² A. C. dos Reis² A. D. Dowling⁶⁹ W. Duan⁷² P. Duda⁸⁰ M. W. Dudek⁴¹ L. Dufour⁴⁹ V. Duk³⁴
 P. Durante⁴⁹ M. M. Duras⁸⁰ J. M. Durham⁶⁸ O. D. Durmus⁷⁷ A. Dziurda⁴¹ A. Dzyuba⁴⁴ S. Easo⁵⁸
 E. Eckstein¹⁸ U. Egede¹ A. Egorychev⁴⁴ V. Egorychev⁴⁴ S. Eisenhardt⁵⁹ E. Ejopu⁶³ L. Eklund⁸²
 M. Elashri⁶⁶ J. Ellbracht¹⁹ S. Ely⁶² A. Ene⁴³ J. Eschle⁶⁹ S. Esen²² T. Evans⁶³ F. Fabiano^{32,m}
 L. N. Falcao² Y. Fan⁷ B. Fang⁷ L. Fantini^{34,49,q} M. Faria⁵⁰ K. Farmer⁵⁹ D. Fazzini^{31,c} L. Felkowski⁸⁰
 M. Feng^{5,7} M. Feo¹⁹ A. Fernandez Casani⁴⁸ M. Fernandez Gomez⁴⁷ A. D. Ferez⁶⁷ F. Ferrari^{25,i}
 F. Ferreira Rodrigues³ M. Ferrillo⁵¹ M. Ferro-Luzzi⁴⁹ S. Filippov⁴⁴ R. A. Fini²⁴ M. Fiorini^{26,f} M. Firllej⁴⁰
 K. L. Fischer⁶⁴ D. S. Fitzgerald⁸³ C. Fitzpatrick⁶³ T. Fiutowski⁴⁰ F. Fleuret¹⁵ M. Fontana²⁵ L. F. Foreman⁶³
 R. Forty⁴⁹ D. Foulds-Holt⁵⁶ V. Franco Lima³ M. Franco Sevilla⁶⁷ M. Frank⁴⁹ E. Franzoso^{26,f} G. Frau⁶³
 C. Frei⁴⁹ D. A. Friday⁶³ J. Fu⁷ Q. Fühling^{19,56,b} Y. Fujii¹ T. Fulghesu¹⁶ E. Gabriel³⁸ G. Galati²⁴
 M. D. Galati³⁸ A. Gallas Torreira⁴⁷ D. Galli^{25,i} S. Gambetta⁵⁹ M. Gandelman³ P. Gandini³⁰ B. Ganie⁶³
 H. Gao⁷ R. Gao⁶⁴ T. Q. Gao⁵⁶ Y. Gao⁸ Y. Gao⁶ Y. Gao⁸ L. M. Garcia Martin⁵⁰ P. Garcia Moreno⁴⁶
 J. García Pardiñas⁴⁹ P. Gardner⁶⁷ K. G. Garg⁸ L. Garrido⁴⁶ C. Gaspar⁴⁹ L. L. Gerken¹⁹ E. Gersabeck⁶³
 M. Gersabeck²⁰ T. Gershon⁵⁷ S. Ghizzo^{29,j} Z. Ghorbanimoghaddam⁵⁵ L. Giambastiani^{33,g} F. I. Giasemis^{16,r}
 V. Gibson⁵⁶ H. K. Giemza⁴² A. L. Gilman⁶⁴ M. Giovannetti²⁸ A. Gioventù⁴⁶ L. Girardey⁶³ C. Giugliano^{26,f}
 M. A. Giza⁴¹ E. L. Gkougkousis⁶² F. C. Glaser^{14,22} V. V. Gligorov^{16,49} C. Göbel⁷⁰ E. Golobardes⁴⁵
 D. Golubkov⁴⁴ A. Golutvin^{62,49,44} S. Gomez Fernandez⁴⁶ W. Gomulka⁴⁰ F. Goncalves Abrantes⁶⁴ M. Goncerz⁴¹
 G. Gong^{4,p} J. A. Gooding¹⁹ I. V. Gorelov⁴⁴ C. Gotti³¹ E. Govorkova⁶⁵ J. P. Grabowski¹⁸
 L. A. Granado Cardoso⁴⁹ E. Graugés⁴⁶ E. Graverini^{50,s} L. Grazette⁵⁷ G. Graziani¹ A. T. Grecu⁴³
 L. M. Greeven³⁸ N. A. Grieser⁶⁶ L. Grillo⁶⁰ S. Gromov⁴⁴ C. Gu¹⁵ M. Guarise²⁶ L. Guerry¹¹ V. Guliaeva⁴⁴
 P. A. Günther²² A.-K. Guseinov⁵⁰ E. Gushchin⁴⁴ Y. Guz^{6,49,44} T. Gys⁴⁹ K. Habermann¹⁸ T. Hadavizadeh¹
 C. Hadjivasiliou⁶⁷ G. Haefeli⁵⁰ C. Haen⁴⁹ G. Hallett⁵⁷ M. M. Halvorsen⁴⁹ P. M. Hamilton⁶⁷ J. Hammerich⁶¹
 Q. Han⁸ X. Han^{22,49} S. Hansmann-Menzemer²² L. Hao⁷ N. Harnew⁶⁴ T. H. Harris¹ M. Hartmann¹⁴
 S. Hashmi⁴⁰ J. He^{7,t} F. Hemmer⁴⁹ C. Henderson⁶⁶ R. D. L. Henderson^{1,57} A. M. Hennequin⁴⁹
 K. Hennessy⁶¹ L. Henry⁵⁰ J. Herd⁶² P. Herrero Gascon²² J. Heuel¹⁷ A. Hicheur³ G. Hijano Mendizabal⁵¹

J. Horswill⁶³ R. Hou⁸ Y. Hou¹¹ N. Howarth⁶¹ J. Hu⁷² W. Hu⁶ X. Hu^{4,p} W. Huang⁷ W. Hulsbergen³⁸
R. J. Hunter⁵⁷ M. Hushchyn⁴⁴ D. Hutchcroft⁶¹ M. Idzik⁴⁰ D. Ilin⁴⁴ P. Ilten⁶⁶ A. Inglessi⁴⁴ A. Iniukhin⁴⁴
A. Ishteev⁴⁴ K. Ivshin⁴⁴ R. Jacobsson⁴⁹ H. Jage¹⁷ S. J. Jaimes Elles^{75,49,48} S. Jakobsen⁴⁹ E. Jans³⁸
B. K. Jashal⁴⁸ A. Jawahery⁶⁷ V. Jevtic^{19,b} E. Jiang⁶⁷ X. Jiang^{5,7} Y. Jiang⁷ Y. J. Jiang⁶ M. John⁶⁴
A. John Rubesh Rajan²³ D. Johnson⁵⁴ C. R. Jones⁵⁶ T. P. Jones⁵⁷ S. Joshi⁴² B. Jost⁴⁹ J. Juan Castella⁵⁶
N. Jurik⁴⁹ I. Juszcak⁴¹ D. Kaminaris⁵⁰ S. Kandybei⁵² M. Kane⁵⁹ Y. Kang^{4,p} C. Kar¹¹ M. Karacson⁴⁹
D. Karpenkov⁴⁴ A. Kauniskangas⁵⁰ J. W. Kautz⁶⁶ M. K. Kazanecki⁴¹ F. Keizer⁴⁹ M. Kenzie⁵⁶ T. Ketel³⁸
B. Khanji⁶⁹ A. Kharisova⁴⁴ S. Kholodenko^{35,49} G. Khreich¹⁴ T. Kirn¹⁷ V. S. Kirsebom^{31,c} O. Kitouni⁶⁵
S. Klaver³⁹ N. Kleijne^{35,e} K. Klimaszewski⁴² M. R. Kmiec⁴² S. Koliiev⁵³ L. Kolk¹⁹ A. Konoplyannikov⁴⁴
P. Kopciwicz⁴⁹ P. Koppenburg³⁸ M. Korolev⁴⁴ I. Kostiuk³⁸ O. Kot⁵³ S. Kotriakhova⁴⁴ A. Kozachuk⁴⁴
P. Kravchenko⁴⁴ L. Kravchuk⁴⁴ M. Kreps⁵⁷ P. Krokovny⁴⁴ W. Krupa⁶⁹ W. Krzemien⁴² O. Kshyvanskyi⁵³
S. Kubis⁸⁰ M. Kucharczyk⁴¹ V. Kudryavtsev⁴⁴ E. Kulikova⁴⁴ A. Kupsc⁸² B. K. Kutsenko¹³ D. Lacarrere⁴⁹
P. Laguarda Gonzalez⁴⁶ A. Lai³² A. Lampis³² D. Lancierini⁵⁶ C. Landesa Gomez⁴⁷ J. J. Lane¹ R. Lane⁵⁵
G. Lanfranchi²⁸ C. Langenbruch²² J. Langer¹⁹ O. Lantwin⁴⁴ T. Latham⁵⁷ F. Lazzari^{35,49,s} C. Lazzeroni⁵⁴
R. Le Gac¹³ H. Lee⁶¹ R. Lefèvre¹¹ A. Leflat⁴⁴ S. Legotin⁴⁴ M. Lehurax⁵⁷ E. Lemos Cid⁴⁹ O. Leroy¹³
T. Lesiak⁴¹ E. D. Lesser⁴⁹ B. Leverington²² A. Li^{4,p} C. Li¹³ H. Li⁷² K. Li⁸ L. Li⁶³ M. Li⁸ P. Li⁷
P.-R. Li⁷³ Q. Li^{5,7} S. Li⁸ T. Li^{5,u} T. Li⁷² Y. Li⁸ Y. Li⁵ Z. Lian^{4,p} X. Liang⁶⁹ S. Libralon⁴⁸ C. Lin⁷
T. Lin⁵⁸ R. Lindner⁴⁹ H. Linton⁶² V. Lisovskyi⁵⁰ R. Litvinov^{32,49} F. L. Liu¹ G. Liu⁷² K. Liu⁷³ S. Liu^{5,7}
W. Liu⁸ Y. Liu⁵⁹ Y. Liu⁷³ Y. L. Liu⁶² G. Loachamin Ordonez⁷⁰ A. Lobo Salvia⁴⁶ A. Loi³² T. Long⁵⁶
J. H. Lopes³ A. Lopez Huertas⁴⁶ S. López Soliño⁴⁷ Q. Lu¹⁵ C. Lucarelli²⁷ D. Lucchesi^{33,g}
M. Lucio Martinez⁷⁹ V. Lukashenko^{38,53} Y. Luo⁶ A. Lupato^{33,v} E. Luppi^{26,f} K. Lynch²³ X.-R. Lyu⁷
G. M. Ma^{4,p} S. Maccolini¹⁹ F. Machefert¹⁴ F. Maciuc⁴³ B. Mack⁶⁹ I. Mackay⁶⁴ L. M. Mackey⁶⁹
L. R. Madhan Mohan⁵⁶ M. J. Madurai⁵⁴ A. Maevskiy⁴⁴ D. Magdalinski³⁸ D. Maisuzenko⁴⁴ M. W. Majewski⁴⁰
J. J. Malczewski⁴¹ S. Malde⁶⁴ L. Malentacca⁴⁹ A. Malinin⁴⁴ T. Maltsev⁴⁴ G. Manca^{32,m} G. Mancinelli¹³
C. Mancuso^{30,14,k} R. Manera Escalero⁴⁶ F. M. Mangarella³⁷ D. Manuzzi²⁵ D. Marangotto^{30,k} J. F. Marchand¹⁰
R. Marchevski⁵⁰ U. Marconi²⁵ E. Mariani¹⁶ S. Mariani⁴⁹ C. Marin Benito^{46,49} J. Marks²² A. M. Marshall⁵⁵
L. Martel⁶⁴ G. Martelli^{34,q} G. Martellotti³⁶ L. Martinazzoli⁴⁹ M. Martinelli^{31,c} D. Martinez Gomez⁷⁸
D. Martinez Santos⁸¹ F. Martinez Vidal⁴⁸ A. Martorell i Granollers⁴⁵ A. Massafferri² R. Matev⁴⁹ A. Mathad⁴⁹
V. Matiunin⁴⁴ C. Matteuzzi⁶⁹ K. R. Mattioli¹⁵ A. Mauri⁶² E. Maurice¹⁵ J. Mauricio⁴⁶ P. Mayencourt⁵⁰
J. Mazorra de Cos⁴⁸ M. Mazurek⁴² M. McCann⁶² L. McConnell²³ T. H. McGrath⁶³ N. T. McHugh⁶⁰
A. McNab⁶³ R. McNulty²³ B. Meadows⁶⁶ G. Meier¹⁹ D. Melnychuk⁴² F. M. Meng^{4,p} M. Merk^{38,79}
A. Merli⁵⁰ L. Meyer Garcia⁶⁷ D. Miao^{5,7} H. Miao⁷ M. Mikhasenko⁷⁶ D. A. Milanese^{75,w} A. Minotti^{31,c}
E. Minucci²⁸ T. Miralles¹¹ B. Mitreska¹⁹ D. S. Mitzel¹⁹ A. Modak⁵⁸ R. A. Mohammed⁶⁴ R. D. Moise¹⁷
S. Mokhnenko⁴⁴ E. F. Molina Cardenas⁸³ T. Mombächer⁴⁹ M. Monk^{57,1} S. Monteil¹¹ A. Morcillo Gomez⁴⁷
G. Morello²⁸ M. J. Morello^{35,e} M. P. Morgenthaler²² J. Moron⁴⁰ W. Morren³⁸ A. B. Morris⁴⁹ A. G. Morris¹³
R. Mountain⁶⁹ H. Mu^{4,p} Z. M. Mu⁶ E. Muhammad⁵⁷ F. Muheim⁵⁹ M. Mulder⁷⁸ K. Müller⁵¹
F. Muñoz-Rojas⁹ R. Murta⁶² P. Naik⁶¹ T. Nakada⁵⁰ R. Nandakumar⁵⁸ T. Nanut⁴⁹ I. Nasteva³
M. Needham⁵⁹ N. Neri^{30,k} S. Neubert¹⁸ N. Neufeld⁴⁹ P. Neustroev⁴⁴ J. Nicolini^{19,14} D. Nicotra⁷⁹
E. M. Niel⁴⁹ N. Nikitin⁴⁴ Q. Niu⁷³ P. Nogarolli³ P. Nogga¹⁸ C. Normand⁵⁵ J. Novoa Fernandez⁴⁷
G. Nowak⁶⁶ C. Nunez⁸³ H. N. Nur⁶⁰ A. Oblakowska-Mucha⁴⁰ V. Obraztsov⁴⁴ T. Oeser¹⁷ S. Okamura^{26,f}
A. Okhotnikov⁴⁴ O. Okhrimenko⁵³ R. Oldeman^{32,m} F. Oliva⁵⁹ M. Olocco¹⁹ C. J. G. Onderwater⁷⁹
R. H. O'Neil⁴⁹ D. Osthus¹⁹ J. M. Otalora Goicochea³ P. Owen⁵¹ A. Oyanguren⁴⁸ O. Ozcelik⁵⁹ F. Paciolla^{35,x}
A. Padee⁴² K. O. Padeken¹⁸ B. Pagare⁵⁷ P. R. Pais²² T. Pajero⁴⁹ A. Palano²⁴ M. Palutan²⁸ X. Pan^{4,p}
G. Panshin⁴⁴ L. Paolucci⁵⁷ A. Papanestis^{58,49} M. Pappagallo^{24,o} L. L. Pappalardo^{26,f} C. Pappenheimer⁶⁶
C. Parkes⁶³ D. Parmar⁷⁶ B. Passalacqua^{26,f} G. Passaleva²⁷ D. Passaro^{35,49,e} A. Pastore²⁴ M. Patel⁶²
J. Patoc⁶⁴ C. Patrignani^{25,i} A. Paul⁶⁹ C. J. Pawley⁷⁹ A. Pellegrino³⁸ J. Peng^{5,7} M. Pepe Altarelli²⁸
S. Perazzini²⁵ D. Pereima⁴⁴ H. Pereira Da Costa⁶⁸ A. Pereiro Castro⁴⁷ P. Perret¹¹ A. Perrevoort⁷⁸
A. Perro^{49,13} M. J. Peters⁶⁶ K. Petridis⁵⁵ A. Petrolini^{29,j} J. P. Pfaller⁶⁶ H. Pham⁶⁹ L. Pica^{35,e} M. Piccini³⁴
L. Piccolo³² B. Pietrzyk¹⁰ G. Pietrzyk¹⁴ R. N. Pilato⁶¹ D. Pinci³⁶ F. Pisani⁴⁹ M. Pizzichemi^{31,49,c}

V. Placinta⁴³, M. Plo Casasus⁴⁷, T. Poeschl⁴⁹, F. Polci¹⁶, M. Poli Lener²⁸, A. Poluektov¹³, N. Polukhina⁴⁴,
 I. Polyakov⁴⁴, E. Polycarpo³, S. Ponce⁴⁹, D. Popov⁷, S. Poslavskii⁴⁴, K. Prasanth⁵⁹, C. Prouve⁸¹,
 D. Provenzano^{32,m}, V. Pugatch⁵³, G. Punzi^{35,s}, S. Qasim⁵¹, Q. Q. Qian⁶, W. Qian⁷, N. Qin^{4,p}, S. Qu^{4,p},
 R. Quagliani⁴⁹, R. I. Rabadan Trejo⁵⁷, J. H. Rademacker⁵⁵, M. Rama³⁵, M. Ramírez García⁸³,
 V. Ramos De Oliveira⁷⁰, M. Ramos Pernas⁵⁷, M. S. Rangel³, F. Ratnikov⁴⁴, G. Raven³⁹, M. Rebollo De Miguel⁴⁸,
 F. Redi^{30,v}, J. Reich⁵⁵, F. Reiss⁶³, Z. Ren⁷, P. K. Resmi⁶⁴, R. Ribatti⁵⁰, G. R. Ricart^{15,12}, D. Riccardi^{35,e},
 S. Ricciardi⁵⁸, K. Richardson⁶⁵, M. Richardson-Slipper⁵⁹, K. Rinnert⁶¹, P. Robbe^{14,49}, G. Robertson⁶⁰,
 E. Rodrigues⁶¹, A. Rodriguez Alvarez⁴⁶, E. Rodriguez Fernandez⁴⁷, J. A. Rodriguez Lopez⁷⁵,
 E. Rodriguez Rodriguez⁴⁷, J. Roensch¹⁹, A. Rogachev⁴⁴, A. Rogovskiy⁵⁸, D. L. Rolf⁴⁹, P. Roloff⁴⁹,
 V. Romanovskiy⁶⁶, A. Romero Vidal⁴⁷, G. Romolini²⁶, F. Ronchetti⁵⁰, T. Rong⁶, M. Rotondo²⁸, S. R. Roy²²,
 M. S. Rudolph⁶⁹, M. Ruiz Diaz²², R. A. Ruiz Fernandez⁴⁷, J. Ruiz Vidal^{82,y}, A. Ryzhikov⁴⁴, J. Ryzka⁴⁰,
 J. J. Saavedra-Arias⁹, J. J. Saborido Silva⁴⁷, R. Sadek¹⁵, N. Sagidova⁴⁴, D. Sahoo⁷⁷, N. Sahoo⁵⁴, B. Saitta^{32,m},
 M. Salomoni^{31,49,c}, I. Sanderswood⁴⁸, R. Santacesaria³⁶, C. Santamarina Rios⁴⁷, M. Santimaria^{28,49}, L. Santoro²,
 E. Santovetti³⁷, A. Saputi^{26,49}, D. Saranin⁴⁴, A. Sarnatskiy⁷⁸, G. Sarpis⁵⁹, M. Sarpis⁶³, C. Satriano^{36,z},
 A. Satta³⁷, M. Saur⁶, D. Savrina⁴⁴, H. Sazak¹⁷, F. Sborzacchi^{49,28}, L. G. Scantlebury Smead⁶⁴, A. Scarabotto¹⁹,
 S. Schael¹⁷, S. Scherl⁶¹, M. Schiller⁶⁰, H. Schindler⁴⁹, M. Schmelling²¹, B. Schmidt⁴⁹, S. Schmitt¹⁷,
 H. Schmitz¹⁸, O. Schneider⁵⁰, A. Schopper⁴⁹, N. Schulte¹⁹, S. Schulte⁵⁰, M. H. Schune¹⁴, R. Schwemmer⁴⁹,
 G. Schwering¹⁷, B. Sciascia²⁸, A. Sciuccati⁴⁹, I. Segal⁷⁶, S. Sellam⁴⁷, A. Semennikov⁴⁴, T. Senger⁵¹,
 M. Senghi Soares³⁹, A. Sergi^{29,j}, N. Serra⁵¹, L. Sestini³³, A. Seuthe¹⁹, Y. Shang¹⁹, D. M. Shangase⁸³,
 M. Shapkin⁴⁴, R. S. Sharma⁶⁹, I. Shchemerov⁴⁴, L. Shchutska⁵⁰, T. Shears⁶¹, L. Shekhtman⁴⁴, Z. Shen⁶,
 S. Sheng^{5,7}, V. Shevchenko⁴⁴, B. Shi⁷, Q. Shi⁷, Y. Shimizu¹⁴, E. Shmanin²⁵, R. Shorkin⁴⁴, J. D. Shupperd⁶⁹,
 R. Silva Coutinho⁶⁹, G. Simi^{33,g}, S. Simone^{24,o}, N. Skidmore⁵⁷, T. Skwarnicki⁶⁹, M. W. Slater⁵⁴,
 J. C. Smallwood⁶⁴, E. Smith⁶⁵, K. Smith⁶⁸, M. Smith⁶², A. Snoch³⁸, L. Soares Lavra⁵⁹, M. D. Sokoloff⁶⁶,
 F. J. P. Soler⁶⁰, A. Solomin^{44,55}, A. Solovev⁴⁴, I. Solovyev⁴⁴, N. S. Sommerfeld¹⁸, R. Song¹, Y. Song⁵⁰,
 Y. Song^{4,p}, Y. S. Song⁶, F. L. Souza De Almeida⁶⁹, B. Souza De Paula³, E. Spadaro Norella^{29,j}, E. Spedicato²⁵,
 J. G. Speer¹⁹, E. Spiridenkov⁴⁴, P. Spradlin⁶⁰, V. Sriskaran⁴⁹, F. Stagni⁴⁹, M. Stahl⁷⁶, S. Stahl⁴⁹, S. Stanislaus⁶⁴,
 M. Stefaniak⁸⁴, E. N. Stein⁴⁹, O. Steinkamp⁵¹, O. Stenyakin⁴⁴, H. Stevens¹⁹, D. Strelakina⁴⁴, Y. Su⁷, F. Suljik⁶⁴,
 J. Sun³², L. Sun⁷⁴, D. Sundfeld², W. Sutcliffe⁵¹, P. N. Swallow⁵⁴, K. Swientek⁴⁰, F. Swystun⁵⁶, A. Szabelski⁴²,
 T. Szumlak⁴⁰, Y. Tan^{4,p}, Y. Tang⁷⁴, M. D. Tat²², A. Terentev⁴⁴, F. Terzuoli^{35,49,x}, F. Teubert⁴⁹, E. Thomas⁴⁹,
 D. J. D. Thompson⁵⁴, H. Tilquin⁶², V. Tisserand¹¹, S. T'Jampens¹⁰, M. Tobin^{5,49}, L. Tomassetti^{26,f},
 G. Tonani^{30,k}, X. Tong⁶, T. Tork³⁰, D. Torres Machado², L. Toscano¹⁹, D. Y. Tou^{4,p}, C. Trippel⁴⁵, G. Tuci²²,
 N. Tuning³⁸, L. H. Uecker²², A. Ukleja⁴⁰, D. J. Unverzagt²², B. Urbach⁵⁹, A. Usachov³⁹, A. Ustyuzhanin⁴⁴,
 U. Uwer²², V. Vagnoni²⁵, V. Valcarce Cadenas⁴⁷, G. Valenti²⁵, N. Valls Canudas⁴⁹, J. van Eldik⁴⁹,
 H. Van Hecke⁶⁸, E. van Herwijnen⁶², C. B. Van Hulse^{47,aa}, R. Van Laak⁵⁰, M. van Veghel³⁸, G. Vasquez⁵¹,
 R. Vazquez Gomez⁴⁶, P. Vazquez Regueiro⁴⁷, C. Vázquez Sierra⁴⁷, S. Vecchi²⁶, J. J. Velthuis⁵⁵, M. Veltri^{27,bb},
 A. Venkateswaran⁵⁰, M. Verdognia³², M. Vesterinen⁵⁷, D. Vico Benet⁶⁴, P. Vidrier Villalba⁴⁶, M. Vieites Diaz⁴⁷,
 X. Vilasis-Cardona⁴⁵, E. Vilella Figueras⁶¹, A. Villa²⁵, P. Vincent¹⁶, F. C. Volle⁵⁴, D. vom Bruch¹³,
 N. Voropaev⁴⁴, K. Vos⁷⁹, C. Vrahas⁵⁹, J. Wagner¹⁹, J. Walsh³⁵, E. J. Walton^{1,57}, G. Wan⁶, C. Wang²²,
 G. Wang⁸, H. Wang⁷³, J. Wang⁶, J. Wang⁵, J. Wang^{4,p}, J. Wang⁷⁴, M. Wang³⁰, N. W. Wang⁷, R. Wang⁵⁵,
 X. Wang⁸, X. Wang⁷², X. W. Wang⁶², Y. Wang⁶, Y. W. Wang⁷³, Z. Wang¹⁴, Z. Wang^{4,p}, Z. Wang³⁰,
 J. A. Ward^{57,1}, M. Waterlaet⁴⁹, N. K. Watson⁵⁴, D. Websdale⁶², Y. Wei⁶, J. Wendel⁸¹, B. D. C. Westhenry⁵⁵,
 C. White⁵⁶, M. Whitehead⁶⁰, E. Whiter⁵⁴, A. R. Wiederhold⁶³, D. Wiedner¹⁹, G. Wilkinson⁶⁴,
 M. K. Wilkinson⁶⁶, M. Williams⁶⁵, M. J. Williams⁴⁹, M. R. J. Williams⁵⁹, R. Williams⁵⁶, Z. Williams⁵⁵,
 F. F. Wilson⁵⁸, M. Winn¹², W. Wislicki⁴², M. Witek⁴¹, L. Witola²², G. Wormser¹⁴, S. A. Wotton⁵⁶, H. Wu⁶⁹,
 J. Wu⁸, X. Wu⁷⁴, Y. Wu⁶, Z. Wu⁷, K. Wyllie⁴⁹, S. Xian⁷², Z. Xiang⁵, Y. Xie⁸, T. X. Xing³⁰, A. Xu³⁵, L. Xu^{4,p},
 L. Xu^{4,p}, M. Xu⁵⁷, Z. Xu⁴⁹, Z. Xu⁷, Z. Xu⁵, K. Yang⁶², S. Yang⁷, X. Yang⁶, Y. Yang^{29,j}, Z. Yang⁶,
 V. Yeroshenko¹⁴, H. Yeung⁶³, H. Yin⁸, X. Yin⁷, C. Y. Yu⁶, J. Yu⁷¹, X. Yuan⁵, Y. Yuan^{5,7}, E. Zaffaroni⁵⁰

M. Zavertyaev²¹, M. Zdybal⁴¹, F. Zenesini²⁵, C. Zeng^{5,7}, M. Zeng^{4,p}, C. Zhang⁶, D. Zhang⁸, J. Zhang⁷,
 L. Zhang^{4,p}, S. Zhang⁷¹, S. Zhang⁶⁴, Y. Zhang⁶, Y. Z. Zhang^{4,p}, Z. Zhang^{4,p}, Y. Zhao²², A. Zhelezov²²,
 S. Z. Zheng⁶, X. Z. Zheng^{4,p}, Y. Zheng⁷, T. Zhou⁶, X. Zhou⁸, Y. Zhou⁷, V. Zhovkovska⁵⁷, L. Z. Zhu⁷,
 X. Zhu^{4,p}, X. Zhu⁸, V. Zhukov¹⁷, J. Zhuo⁴⁸, Q. Zou^{5,7}, D. Zuliani^{33,g} and G. Zunica⁵⁰

(LHCb Collaboration)

¹*School of Physics and Astronomy, Monash University, Melbourne, Australia*

²*Centro Brasileiro de Pesquisas Físicas (CBPF), Rio de Janeiro, Brazil*

³*Universidade Federal do Rio de Janeiro (UFRJ), Rio de Janeiro, Brazil*

⁴*Department of Engineering Physics, Tsinghua University, Beijing, China*

⁵*Institute Of High Energy Physics (IHEP), Beijing, China*

⁶*School of Physics State Key Laboratory of Nuclear Physics and Technology, Peking University, Beijing, China*

⁷*University of Chinese Academy of Sciences, Beijing, China*

⁸*Institute of Particle Physics, Central China Normal University, Wuhan, Hubei, China*

⁹*Consejo Nacional de Rectores (CONARE), San Jose, Costa Rica*

¹⁰*Université Savoie Mont Blanc, CNRS, IN2P3-LAPP, Annecy, France*

¹¹*Université Clermont Auvergne, CNRS/IN2P3, LPC, Clermont-Ferrand, France*

¹²*Université Paris-Saclay, Centre d'Etudes de Saclay (CEA), IRFU, Saclay, Gif-Sur-Yvette, France*

¹³*Aix Marseille Univ, CNRS/IN2P3, CPPM, Marseille, France*

¹⁴*Université Paris-Saclay, CNRS/IN2P3, IJCLab, Orsay, France*

¹⁵*Laboratoire Leprince-Ringuet, CNRS/IN2P3, Ecole Polytechnique, Institut Polytechnique de Paris, Palaiseau, France*

¹⁶*LPNHE, Sorbonne Université, Paris Diderot Sorbonne Paris Cité, CNRS/IN2P3, Paris, France*

¹⁷*I. Physikalisches Institut, RWTH Aachen University, Aachen, Germany*

¹⁸*Universität Bonn - Helmholtz-Institut für Strahlen und Kernphysik, Bonn, Germany*

¹⁹*Fakultät Physik, Technische Universität Dortmund, Dortmund, Germany*

²⁰*Physikalisches Institut, Albert-Ludwigs-Universität Freiburg, Freiburg, Germany*

²¹*Max-Planck-Institut für Kernphysik (MPIK), Heidelberg, Germany*

²²*Physikalisches Institut, Ruprecht-Karls-Universität Heidelberg, Heidelberg, Germany*

²³*School of Physics, University College Dublin, Dublin, Ireland*

²⁴*INFN Sezione di Bari, Bari, Italy*

²⁵*INFN Sezione di Bologna, Bologna, Italy*

²⁶*INFN Sezione di Ferrara, Ferrara, Italy*

²⁷*INFN Sezione di Firenze, Firenze, Italy*

²⁸*INFN Laboratori Nazionali di Frascati, Frascati, Italy*

²⁹*INFN Sezione di Genova, Genova, Italy*

³⁰*INFN Sezione di Milano, Milano, Italy*

³¹*INFN Sezione di Milano-Bicocca, Milano, Italy*

³²*INFN Sezione di Cagliari, Monserrato, Italy*

³³*INFN Sezione di Padova, Padova, Italy*

³⁴*INFN Sezione di Perugia, Perugia, Italy*

³⁵*INFN Sezione di Pisa, Pisa, Italy*

³⁶*INFN Sezione di Roma La Sapienza, Roma, Italy*

³⁷*INFN Sezione di Roma Tor Vergata, Roma, Italy*

³⁸*Nikhef National Institute for Subatomic Physics, Amsterdam, Netherlands*

³⁹*Nikhef National Institute for Subatomic Physics and VU University Amsterdam, Amsterdam, Netherlands*

⁴⁰*AGH - University of Krakow, Faculty of Physics and Applied Computer Science, Kraków, Poland*

⁴¹*Henryk Niewodniczanski Institute of Nuclear Physics Polish Academy of Sciences, Kraków, Poland*

⁴²*National Center for Nuclear Research (NCBJ), Warsaw, Poland*

⁴³*Horia Hulubei National Institute of Physics and Nuclear Engineering, Bucharest-Magurele, Romania*

⁴⁴*Authors affiliated with an institute formerly covered by a cooperation agreement with CERN*

⁴⁵*DS4DS, La Salle, Universitat Ramon Llull, Barcelona, Spain*

⁴⁶*ICCUB, Universitat de Barcelona, Barcelona, Spain*

⁴⁷*Instituto Galego de Física de Altas Enerxías (IGFAE), Universidade de Santiago de Compostela, Santiago de Compostela, Spain*

⁴⁸*Instituto de Física Corpuscular, Centro Mixto Universidad de Valencia - CSIC, Valencia, Spain*

⁴⁹*European Organization for Nuclear Research (CERN), Geneva, Switzerland*

⁵⁰*Institute of Physics, Ecole Polytechnique Fédérale de Lausanne (EPFL), Lausanne, Switzerland*

⁵¹*Physik-Institut, Universität Zürich, Zürich, Switzerland*

- ⁵²*NSC Kharkiv Institute of Physics and Technology (NSC KIPT), Kharkiv, Ukraine*
- ⁵³*Institute for Nuclear Research of the National Academy of Sciences (KINR), Kyiv, Ukraine*
- ⁵⁴*School of Physics and Astronomy, University of Birmingham, Birmingham, United Kingdom*
- ⁵⁵*H.H. Wills Physics Laboratory, University of Bristol, Bristol, United Kingdom*
- ⁵⁶*Cavendish Laboratory, University of Cambridge, Cambridge, United Kingdom*
- ⁵⁷*Department of Physics, University of Warwick, Coventry, United Kingdom*
- ⁵⁸*STFC Rutherford Appleton Laboratory, Didcot, United Kingdom*
- ⁵⁹*School of Physics and Astronomy, University of Edinburgh, Edinburgh, United Kingdom*
- ⁶⁰*School of Physics and Astronomy, University of Glasgow, Glasgow, United Kingdom*
- ⁶¹*Oliver Lodge Laboratory, University of Liverpool, Liverpool, United Kingdom*
- ⁶²*Imperial College London, London, United Kingdom*
- ⁶³*Department of Physics and Astronomy, University of Manchester, Manchester, United Kingdom*
- ⁶⁴*Department of Physics, University of Oxford, Oxford, United Kingdom*
- ⁶⁵*Massachusetts Institute of Technology, Cambridge, Massachusetts, USA*
- ⁶⁶*University of Cincinnati, Cincinnati, Ohio, USA*
- ⁶⁷*University of Maryland, College Park, Maryland, USA*
- ⁶⁸*Los Alamos National Laboratory (LANL), Los Alamos, New Mexico, USA*
- ⁶⁹*Syracuse University, Syracuse, New York, USA*
- ⁷⁰*Pontificia Universidade Católica do Rio de Janeiro (PUC-Rio), Rio de Janeiro, Brazil
(associated with Universidade Federal do Rio de Janeiro (UFRJ), Rio de Janeiro, Brazil)*
- ⁷¹*School of Physics and Electronics, Hunan University, Changsha City, China
(associated with Institute of Particle Physics, Central China Normal University, Wuhan, Hubei, China)*
- ⁷²*Guangdong Provincial Key Laboratory of Nuclear Science, Guangdong-Hong Kong Joint Laboratory of Quantum Matter,
Institute of Quantum Matter, South China Normal University, Guangzhou, China
(associated with Department of Engineering Physics, Tsinghua University, Beijing, China)*
- ⁷³*Lanzhou University, Lanzhou, China
(associated with Institution #5)*
- ⁷⁴*School of Physics and Technology, Wuhan University, Wuhan, China
(associated with Department of Engineering Physics, Tsinghua University, Beijing, China)*
- ⁷⁵*Departamento de Física, Universidad Nacional de Colombia, Bogota, Colombia
(associated with LPNHE, Sorbonne Université, Paris Diderot Sorbonne Paris Cité, CNRS/IN2P3, Paris, France)*
- ⁷⁶*Ruhr Universitaet Bochum, Fakultät f. Physik und Astronomie, Bochum, Germany
(associated with Fakultät Physik, Technische Universität Dortmund, Dortmund, Germany)*
- ⁷⁷*Eotvos Lorand University, Budapest, Hungary
(associated with European Organization for Nuclear Research (CERN), Geneva, Switzerland)*
- ⁷⁸*Van Swinderen Institute, University of Groningen, Groningen, Netherlands
(associated with Nikhef National Institute for Subatomic Physics, Amsterdam, Netherlands)*
- ⁷⁹*Universiteit Maastricht, Maastricht, Netherlands
(associated with Nikhef National Institute for Subatomic Physics, Amsterdam, Netherlands)*
- ⁸⁰*Tadeusz Kosciuszko Cracow University of Technology, Cracow, Poland
(associated with Henryk Niewodniczanski Institute of Nuclear Physics Polish Academy of Sciences, Kraków, Poland)*
- ⁸¹*Universidad da Coruña, A Coruña, Spain
(associated with DS4DS, La Salle, Universitat Ramon Llull, Barcelona, Spain)*
- ⁸²*Department of Physics and Astronomy, Uppsala University, Uppsala, Sweden
(associated with School of Physics and Astronomy, University of Glasgow, Glasgow, United Kingdom)*
- ⁸³*University of Michigan, Ann Arbor, Michigan, USA
(associated with Syracuse University, Syracuse, New York, USA)*
- ⁸⁴*Ohio State University, Columbus, USA
(associated with Los Alamos National Laboratory (LANL), Los Alamos, New Mexico, USA)*

^aDeceased.

^bAlso at Lamarr Institute for Machine Learning and Artificial Intelligence, Dortmund, Germany.

^cAlso at Università degli Studi di Milano-Bicocca, Milano, Italy.

^dAlso at Università di Roma Tor Vergata, Roma, Italy.

^eAlso at Scuola Normale Superiore, Pisa, Italy.

^fAlso at Università di Ferrara, Ferrara, Italy.

^gAlso at Università di Padova, Padova, Italy.

^hAlso at Facultad de Ciencias Físicas, Madrid, Spain.

ⁱAlso at Università di Bologna, Bologna, Italy.

^jAlso at Università di Genova, Genova, Italy.

- ^kAlso at Università degli Studi di Milano, Milano, Italy.
- ^lAlso at Universidad Nacional Autónoma de Honduras, Tegucigalpa, Honduras.
- ^mAlso at Università di Cagliari, Cagliari, Italy.
- ⁿAlso at Centro Federal de Educação Tecnológica Celso Suckow da Fonseca, Rio De Janeiro, Brazil.
- ^oAlso at Università di Bari, Bari, Italy.
- ^pAlso at Center for High Energy Physics, Tsinghua University, Beijing, China.
- ^qAlso at Università di Perugia, Perugia, Italy.
- ^rAlso at LIP6, Sorbonne Université, Paris, France.
- ^sAlso at Università di Pisa, Pisa, Italy.
- ^tAlso at Hangzhou Institute for Advanced Study, UCAS, Hangzhou, China.
- ^uAlso at School of Physics and Electronics, Henan University, Kaifeng, China.
- ^vAlso at Università di Bergamo, Bergamo, Italy.
- ^wAlso at Universidad de Ingeniería y Tecnología (UTEC), Lima, Peru.
- ^xAlso at Università di Siena, Siena, Italy.
- ^yAlso at Department of Physics/Division of Particle Physics, Lund, Sweden.
- ^zAlso at Università della Basilicata, Potenza, Italy.
- ^{aa}Also at Universidad de Alcalá, Alcalá de Henares, Spain.
- ^{bb}Also at Università di Urbino, Urbino, Italy.